

# Activated Biochar from *Gracilaria Edulis* Seaweeds: A Novel Biosorbent for Efficient Uranium Ion Removal in Wastewater Treatment

Titus S<sup>1\*</sup>, Karthick L<sup>2</sup>, Kiruba S<sup>3</sup>, Srithar A<sup>4</sup>, Harish Kumar<sup>5</sup>, Karuna M S<sup>6</sup>

<sup>1\*</sup>Department of Science and Humanities (Chemistry), Jeppiaar Engineering College, Chennai, Tamil Nadu 600119, India (drtitus7071@gmail.com)

<sup>2</sup>Department of Mechanical Engineering, Hindusthan College of Engineering and Technology, Coimbatore, Tamil Nadu 641032, India (bemechkarthick@gmail.com)

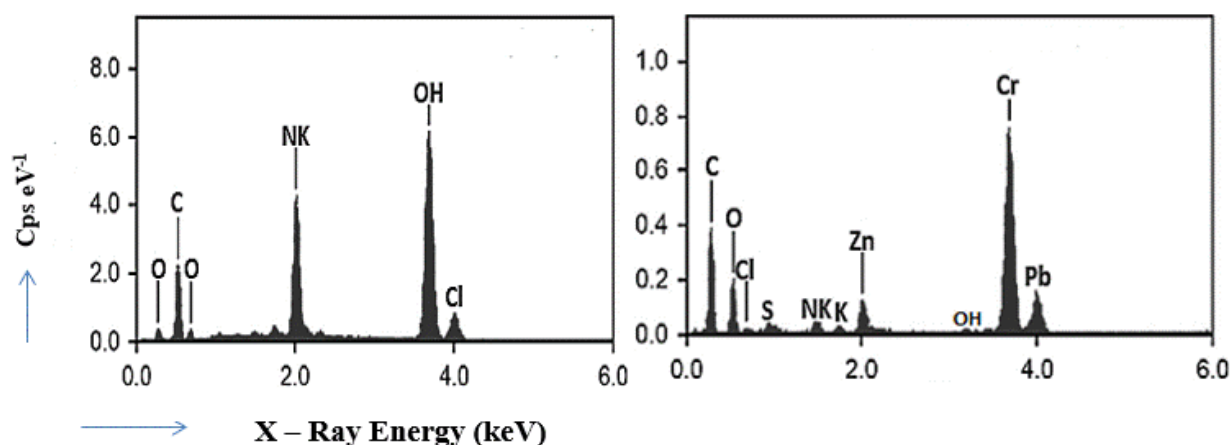
<sup>3</sup>Department of Physics, St. Joseph's College of Engineering, Chennai, Tamil Nadu 600119, India (kirubas@stjosephs.ac.in)

<sup>4</sup>Department of Mechanical Engineering, Sri Sairam Institute of Technology, Chennai, Tamil Nadu 600044, India (asrithar1972@gmail.com)

<sup>5</sup>Department of Chemical Engineering, M.J.P. Rohilkhand University, Bareilly, Uttar Pradesh 243006, India (harishkumar@mnnit.ac.in)

<sup>6</sup>Department of Chemical Engineering, M.J.P. Rohilkhand University, Bareilly, Uttar Pradesh 243006, India (m.karuna@mjpru.ac.in)

## GRAPHICAL ABSTRACT



## ABSTRACT

The biosorption of uranium ions was explored through batch studies employing activated biochar derived from *Gracilaria Edulis* seaweeds. A chemical synthesis approach utilizing concentrated sulfuric acid created and activated the adsorbent material. SEM and FTIR measurements were used to characterize the adsorbent material, and EDX examination validated the adsorption of contaminants. The pH of the uranium-containing solution and the other parameters of reaction time,

dose of biochar, concentration of uranium ions, and solution's temperature were adjusted, and the impact of uranium ion adsorption efficiency was investigated. The adsorption nature and its process were analyzed using various kinetic and equilibrium studies. Metal absorption by the adsorbent is endothermic, according to thermodynamic experiments. Around 93.27% of uranium, and metal ions were recovered in an elution study by adding sulfuric acid in 0.3N. In summary, this study achieved an efficiency of 91.27% for uranium ions from the aqueous solutions using *Gracilaria Edulis* charcoal material as the adsorbent.

**Keywords:** Adsorption, *Gracilaria Edulis*, Uranium, Kinetics, Thermodynamics, Desorption.

## 1. INTRODUCTION

Uranium, a naturally occurring radioactive element, possesses a specific density of  $19 \text{ g/cm}^3$  and exists in various chemical and physical forms within the Earth's crust. Uranium metal ions refer to ions of uranium in its metallic state, typically existing as  $\text{U}^{2+}$ ,  $\text{U}^{3+}$ , or  $\text{U}^{4+}$  ions. These ions result from the chemical oxidation states that uranium can adopt. In various environments, uranium may exist as ions with different charges, and its behaviour is influenced by factors such as pH, redox conditions, and the presence of ligands (Priya et al, 2022). Understanding the behaviour of uranium metal ions is crucial in contexts such as environmental science, nuclear engineering, and studies related to the toxicology of uranium exposure. Uranium can be released into the surrounding environment through various natural and human activities. Some of the primary sources of uranium release include Natural weathering, mining operations, industrial processes, nuclear power plants natural decay etc. Once released, uranium can enter water sources, soil, and the air, potentially impacting ecosystems and posing risks to human health if exposure occurs (Feszterová et al, 2021). The pathways of release and the environmental impact depend on factors such as the form of uranium, local geological conditions, and human activities in the area. Uranium and its derivatives are radioactive and poisonous, creating severe pollution and environmental hazards. Uranium can contaminate drinking water and food, becoming a source of human consumption and causing severe liver, renal, and bone disorders. Bioaccumulation refers to the process by which substances, in this case, uranium, accumulate in living organisms over time. This accumulation can occur as uranium moves through the food chain. Excessive uranium consumption provides a substantial danger of bodily deformities and a variety of disorders (Ambaye et al, 2021). The complex behaviour of uranium in the bloodstream and its potential health effects depend on its chemical forms and interactions with biological molecules. It's important to note that the toxicity of uranium is influenced by factors such as the chemical form of uranium, its concentration, duration of exposure, and

individual susceptibility. Monitoring and understanding these interactions are crucial for assessing the potential health risks associated with uranium exposure. Although cells may repair themselves to some extent when not exposed to enough light, modest morphological alterations with unknown effects have been found (Venkatraman et al, 2021). Beyond nephrotoxicity, there is likely evidence of uranium-induced toxicities in both animals and humans, including carcinogenicity, neurotoxicity, and reproductive toxicity.

Uranium toxicity has been linked to several adverse effects on cellular and molecular levels, including Enhanced Oxidative Damage etc. These effects suggest that uranium can have a range of impacts at the cellular and molecular levels, potentially leading to disruptions in cellular function and overall physiological processes. Understanding these mechanisms is crucial for assessing the risks associated with uranium exposure and developing strategies for mitigating its toxic effects (Haro et al, 2021). It's important to note that the specific mechanisms and outcomes may vary depending on factors such as the chemical form of uranium, concentration, and duration of exposure (Amit Kumar et al, 2022). Human exposure occurs via food, drink, and inhalation, with inhalation exposure deemed negligible. Uranium levels in everyday meals like fresh vegetables and bread were approximately 2 g/kg. The uranium level of other meals, such as meat and rice, ranges from 0.1 to 0.2 g/kg. Indeed, the removal of uranium from contaminated areas is crucial to adhere to regulatory compliance guidelines and ensure environmental safety. This is particularly important due to the potential health and environmental risks associated with uranium exposure. Various technologies, such as adsorption, membrane filtration, ion exchange, and membrane separation, have been employed to eliminate uranium from the aqueous medium (Zhang et al, 2019). Adsorption technology is extensively employed for pollutant removal in various applications, owing to its high efficiency, low cost, and low maintenance requirements (Sheeja et al, 2021). Different adsorbents, including natural minerals and synthesized materials, are explored for their potential application in removing uranium from aqueous solutions. Ongoing research aims to develop novel adsorbents that are not only highly effective in uranium removal but also eco-friendly and cost-effective. The study mentioned earlier specifically investigates the usage of *Gracilaria Edulis* seaweed biosorbent for uranium removal, exploring various parameters to optimize the adsorption process.

## **2. MATERIALS AND METHODS**

### **2.1 Preparation of Biosorbent and Uranium solution**

Collecting *Gracilaria Edulis* (GE) from various sites surrounding Rameswaram and Thoothukudi begins the process. After collecting the seaweed, it is cleaned and sun-dried for 24 hours. It is chopped into little pieces after drying and subjected to continual crushing. 10 grams of GE biosorbent was taken and allowed into continuous carbonization by adding 10 mg of citric acid

followed by thermal heating up to 225 degrees Celsius. Following the carbonization process, the GE biochar is carefully cleaned with double-distilled water and dehydrated for half a day in a hot air oven at 200°C. The hydro charcoal powder is soaked in the H<sub>2</sub>O<sub>2</sub> solution for 24 hours before being heated further in an oven. The resultant sample is collected, rinsed several times with distilled water, and then used in the following experiments. Under room temperature, the synthetic solution was prepared by dissolving uranium nitrate salt (UO<sub>2</sub>(NO<sub>3</sub>)<sub>2</sub>·6H<sub>2</sub>O) in 1000 mg/L proportion using double distilled water. The dissolved uranium ions and their concentration in the synthetic solution were assessed by Atomic Adsorption Spectroscopy (AAS - AA6300 made in Shimadzu, Japan).

## 2.2 Characterization of Biosorbent

The surface morphology of the *Gracilaria Edulis* (GE) biosorbent was examined utilizing a scanning electron microscope (SEM) coupled with Energy Dispersive X-ray Spectroscopy (EDX). With the acceleration of 10 – 20 kV, the SEM was operated and the diameter of the beam was set at 1- 2 mm in 60 – 120 seconds of counting time. The functional groups of GE biosorbent were examined by FTIR peak studies. This analysis was carried out with the help of a Bruker VERTEX and a Platinum Diamond Attenuated Total Reflectance accessory. This ATR attachment has a diamond disc as an internal reflector, allowing observations in the 4000-400 cm<sup>-1</sup> range with a resolution of 4 cm<sup>-1</sup> and a refractive index of 2.4.

## 2.3 pH -Zero Point Change (ZPC)

The pH ZPC is a characteristic property of a material's surface, especially when dealing with adsorbents or sorbents like biosorbents. The pH ZPC is the pH at which the surface of a material carries no net electrical charge. At this point, the material is electrically neutral. For biosorbents or adsorbents, understanding the pH<sub>ZPC</sub> is crucial in predicting the material's behaviour in different pH environments, particularly in aqueous solutions. It influences the adsorption or desorption of ions onto or from the material's surface (Nadir Khan et al, 2020). When the pH of the solution is below the pH<sub>ZPC</sub>, the surface tends to be positively charged, attracting negatively charged ions. Conversely, when the pH is above the pH<sub>ZPC</sub>, the surface tends to be negatively charged, attracting positively charged ions. In the context of uranium, removal using *Gracilaria Edulis* (GE) biosorbent, knowing the pH<sub>ZPC</sub> would be relevant to understanding the optimal pH conditions for efficient biosorption of uranium ions onto the biosorbent surface. The pH at Zero Point Charge (pH<sub>ZPC</sub>) of the *Gracilaria Edulis* (GE) biosorbent was measured at 298 K using a degassed 0.01 M NaCl solution. The procedure includes setting up 100-mL conical flasks containing 50 mL of 0.01 M NaCl solution. Each solution's pH was changed from 2 to 14 by adding 0.5 M HCl. Subsequently, 50 mg of GE biosorbent was

introduced into each pH-adjusted solution, and the mixture was allowed to equilibrate for 24 hours. After the 24-hour equilibration period, the final pH values were measured, and the difference between the initial and final pH values, denoted as  $\Delta\text{pH}$ , was plotted against the initial pH values. The  $\text{pH}_{\text{ZPC}}$  values were determined from the plot where the pH equalled zero, signifying that the biosorbent surface carries no net charge at that particular pH. This approach gives insight into the surface charge properties of the biosorbent, which is necessary for predicting its behaviour in procedures such as uranium ion removal from aqueous solutions.

## 2.4 Batch studies for Uranium adsorption

A batch approach was used to evaluate uranium adsorption on the *Gracilaria Edulis* (GE) adsorbent. The adsorption process was explored under different experimental conditions by altering the solution's pH, reaction time, GE dose, Uranium concentration and temperature. For the adsorption experiments, a specific quantity of powdered *Gracilaria Edulis* (GE) was mixed with 10 mL of uranium nitrate solution, with uranium concentrations ranging from 10 to 50 mg/L. These combinations were shaken in 50 mL well-sealed polypropylene bottles at various pH levels (2–12) and temperatures (25–65°C). The adsorbent dosage and contact duration were adjusted from 0.5 to 3.0 gm, and 10 - 60 minutes respectively. The pH adjustments were made by adding the minimum amount of 0.1 mol/L of HCl and NaOH solutions. The shaking speed of 200 rpm was constantly maintained throughout the adsorption studies. The adsorption efficiency, which represents the fraction of metal ion elimination, was computed using the equation 1:

$$q_u = (C_i - C_f) \frac{V}{m} \quad (1)$$

Equation 2 can be used to find the coefficient of distribution between the bulk phase and solid phase in uranium adsorption.

$$K_d = (C_i - C_f)V/C_i m \quad (2)$$

The final adsorption efficiency for uranium metal ion removal using GE was calculated using equation 3.

$$\% \text{ Adsorption} = \frac{C_f - C_i}{C_f} \times 100 \quad (3)$$

The concentration of uranium ions during the initial time was denoted by  $C_i$ , Final concentration of uranium ions was denoted by  $C_f$ . Solution's volume was denoted by  $V$ , and the mass of the adsorbent was denoted by  $m$ .

## 2.5 Equilibrium modelling

Equilibrium modelling in a batch adsorption process involves developing mathematical models to describe the relationship between the adsorbate (e.g., metal ions) and the adsorbent (e.g., algal biomass) at the point of equilibrium. The purpose is to understand and quantify the distribution

of adsorbate molecules between the liquid phase and the adsorbent surface (Singh et al, 2018). Common equilibrium models used in batch adsorption processes include:

- a) **Langmuir isotherm model** :Assumes monolayer adsorption, suggesting that adsorption occurs on specific sites and that once a site is occupied, no further adsorption can take place (wang et al, 2020). The Langmuir isotherm equation is given by equation 4.

$$\frac{C_e}{q_e} = \frac{1}{q_m} + \frac{1}{q_m k_L} \quad (4)$$

The adsorbate equilibrium concentration was denoted by  $C_e$ , the adsorbed amount of adsorbate during the equilibrium time was denoted by  $q_e$  and the adsorption capacity was denoted by  $q_m$ . and  $K_L$  is the Langmuir adsorption constant.

- b) **Freundlich isotherm model** :The Freundlich isotherm is an empirical model used to describe the adsorption of solutes onto a solid surface. It is often applied to heterogeneous surfaces where multiple layers of adsorption can occur. The Freundlich isotherm equation is given by equation 5.

$$q_e = K_F C_e^{\frac{1}{n}} \quad (5)$$

The constant of the Freundlich model was denoted by  $K_F$  and the exponent of this model was denoted by  $n$ .

- c) **Dubinin-Radushkevich (D-R) Isotherm Model** :the gases on the heterogeneous surface in the adsorbent was described using the D-R isothermal model. It can also be applied to describe the adsorption of solutes in liquid phases on porous adsorbents. The D-R isotherm equation is given by equation 6.

$$\ln q_e = \ln q_D - \beta \epsilon^2 \quad (6)$$

Where  $q_D$  is the Dubinin-Radushkevich adsorption capacity,  $\beta$  is a constant related to the mean free energy of adsorption and  $\epsilon$  is the Polanyi potential.

These models are fitted to experimental data to determine the model parameters, providing insights into the adsorption behaviour and mechanisms of the system at equilibrium.

## 2.6 Kinetic modelling

Kinetic modelling in a batch adsorption process involves developing mathematical models to describe the rate at which adsorption occurs over time. This helps in understanding and predicting the dynamic behaviour of the adsorption process (Su et al, 2021). Common kinetic models used in batch adsorption studies include:

- a) **Pseudo-First order model (Lagergren's Model)** :The main assumption of this model is the electrostatic attraction between uranium ions and the external surface of the GE biosorbent is

likely to follow a physical adsorption mechanism. Equation 7 describes the mathematical expression of this model.

$$\ln(q_e - q_t) = \ln q_e - \frac{k_1}{2.303} t \quad (7)$$

Here  $q_e$  and  $q_t$  represent the amount of uranium ions adsorbed in the given time  $t$  and  $K_1$  represents the constant of the first-order model.

- b) Pseudo-second order model :** The Pseudo-Second-Order Model is a kinetic model commonly used to describe the adsorption process in a batch system. Unlike the Pseudo-First-order model, this model assumes that the rate-limiting step is not only the adsorption to vacant sites but also involves chemical interactions between the adsorbate and adsorbent. Equation 8 describes the mathematical expression of this model.

$$\frac{t}{q_t} = \frac{1}{k_2 q_e^2} + \frac{t}{q_e} \quad (8)$$

Here,  $K_2$  represents the rate constant of this model.

- c) Elovich model :** The Elovich kinetic model is a mathematical model usually active to define the kinetics of metal ion biosorption in a batch system. It assumes a multistep process, including chemisorption involving an interface among the adsorbate and the adsorbent surface. Equation 9 describes the mathematical expression of this model.

$$q_t = \frac{1}{\beta} \ln(\alpha\beta t + 1) \quad (9)$$

The rate of initial adsorption was denoted by  $\alpha$  and the Elovich model constant was denoted by  $\beta$

These models are fitted to experimental data, and the parameters are determined to understand the kinetics of the adsorption process, such as the adsorption rate, mechanism, and controlling steps.

### 3. RESULTS AND DISCUSSION

#### 3.1 SEM analysis of the biosorbent

Figures 1(a) and 1(b) show activated biochar GE powder before and after uranium metal absorption at different levels of working distances. In its initial state (Figure 1a), the adsorbent's surface exhibits numerous active sites and uneven pores, making it conducive to the absorption of contaminants from the aqueous medium. The SEM picture (Figure 1b) reveals that active sites and pores are filled with contaminants after exposure to a uranium ion-containing solution, producing a cloud on the adsorbent surface. No additional changes are detected after reaching the saturation point, marking the end of the adsorption process (Aydina et al, 2021). This visual inspection provides additional confirmation of the occurrence of pollutants on the activated GE's surface. To further assess the efficiency of targeted metal ion removal and its presence, EDX analysis was employed.

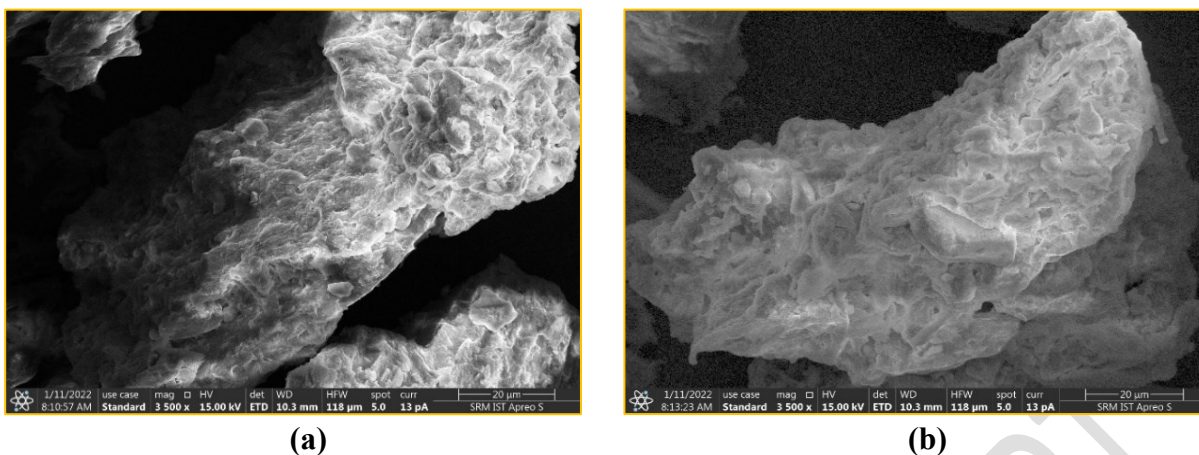


**Figure 1 SEM images of GE biosorbent (a) Raw biosorbent and (b) Uranium adsorbed biosorbent**

### 3.2 EDX analysis

Individual EDX studies were performed to confirm the presence of specific metal ions in laboratory-synthesized solutions under various circumstances. The EDX picture of the raw GE Biochar adsorbent in Figure 2a shows both organic and inorganic components. Figure 2b illustrates the GE biosorbent after the initiation with hydrogen peroxide following the production of biochar. In Figure 2a, elements such as silica, carbon, and oxygen are evident, while Figure 2b reveals the presence of additional contaminants such as uranium and aluminium. Synthetic solutions containing uranium ions were supplied to the activated charcoal adsorbent to determine its ability to adsorb metal ions. The figure shows the EDX depiction of the activated biochar adsorbent after absorbing metal ions during aqueous medium decontamination (Konicki et al, 2017). This study reveals the presence of additional organic and inorganic components, including magnesium, silicon, and iron.

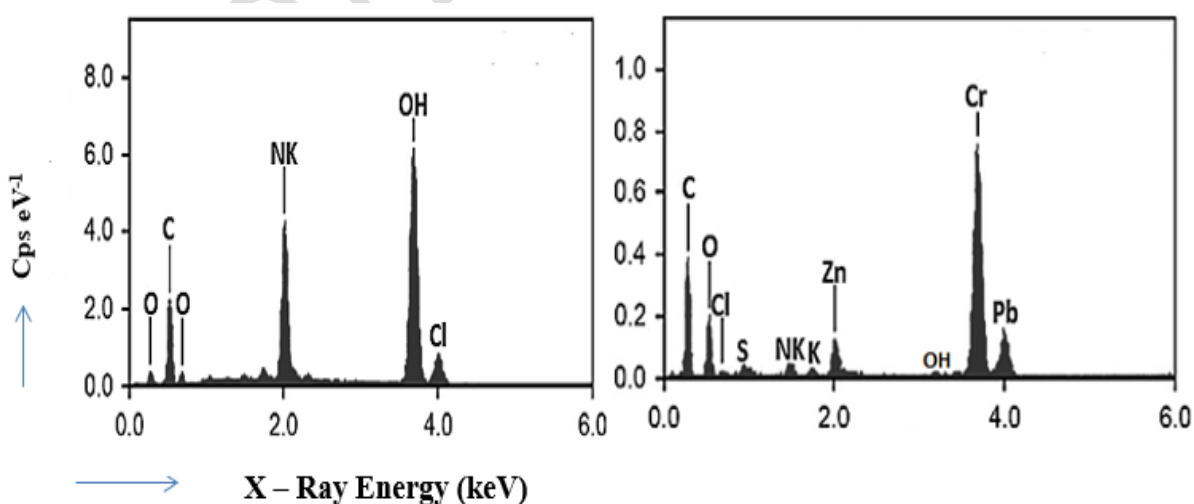
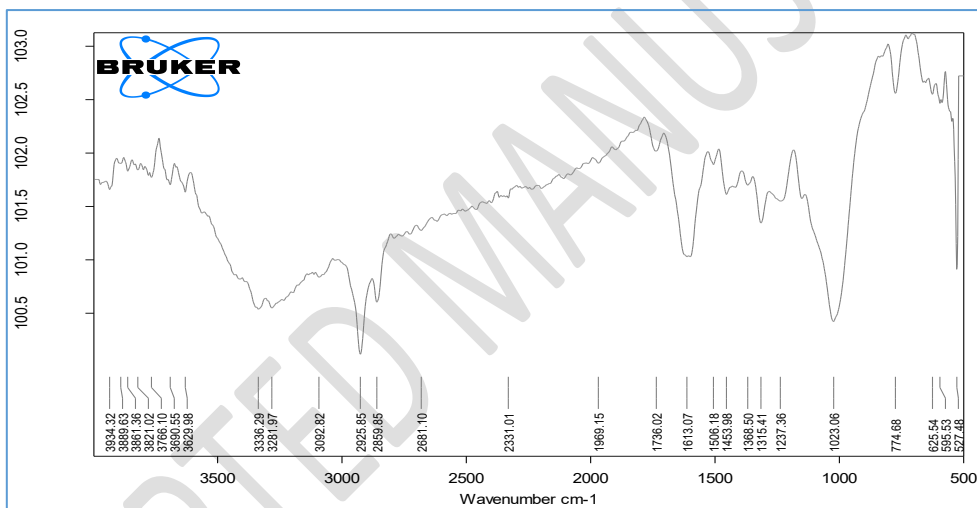


**Figure 2 EDX plot of GE (a) Before and (b) After the adsorption of metal ions**

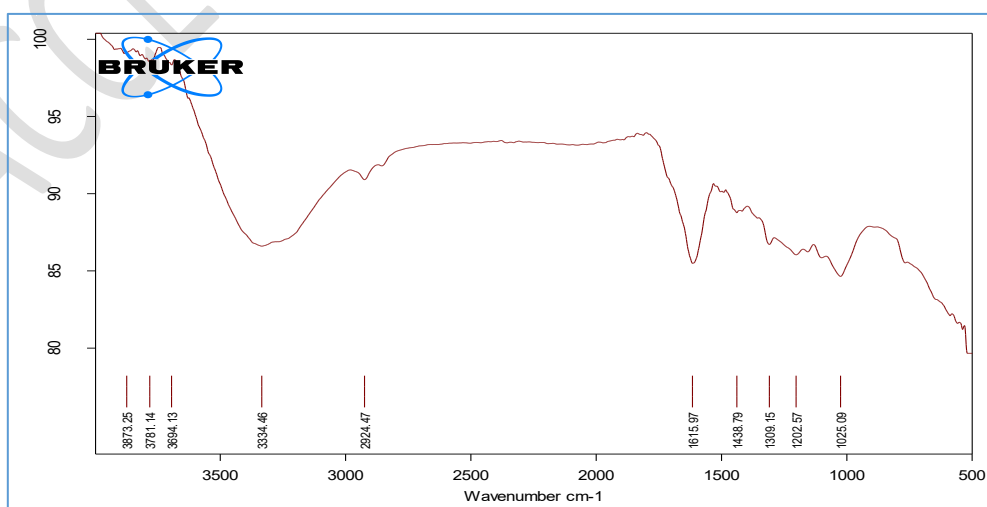
### 3.3 FTIR studies



The FTIR functional groups of the GE adsorbent and the acid-activated adsorbent are shown in Figures 3(a) and 3(b), respectively. The presence of a spectrum of functional clusters was investigated by utilizing bandwidths in energy regions to acquire a better understanding of the adsorption process. The FTIR spectrum displays a high-energy area with bandwidths of  $3766\text{ cm}^{-1}$  and  $3629\text{ cm}^{-1}$ , suggesting the occurrence of efficient groups -OH and N-H. Between  $1738$  and  $1023\text{ cm}^{-1}$ , many functional groups were discovered, including water at  $1620\text{ cm}^{-1}$ , aromatic vibrations between  $1600$  and  $1400\text{ cm}^{-1}$ , -CH<sub>2</sub> bending vibrations between  $1400$  and  $1380\text{ cm}^{-1}$ , and C-O vibrations at  $1080\text{ cm}^{-1}$ . Aromatic vibrations caused by -C-H bending were detected with a bandwidth of  $774\text{ cm}^{-1}$  (Eleryan et al, 2022). Lower-frequency aromatic ring vibrations contributed to -OH stretching, while O-H stretching vibrations stopped at  $2924\text{ cm}^{-1}$ . Finally, FTIR measurements confirmed a wide range of organic and inorganic functional components in the activated GE Biochar adsorbent material. It also demonstrated the adsorbent's capacity to remove pollutants from liquid environments via adsorption.



(a)



(b)

### **Figure 3 FTIR studies of GE biosorbent before and after taking up of metal ions**

#### **3.4 Effect of pH in uranium adsorption**

Because of its effect on the surface characteristics of the adsorbent and the ionization of uranium ions, the pH of the synthetic solution is critical in regulating the removal efficiency of uranium ions from polluted wastewater. pH is an essential element in the adsorption process because it influences both the surface characteristics of the adsorbent and the ionic states of metal ions in solution. The pH range was changed from 2.0 to 10. At the same time, other parameters were kept constant, such as uranium concentration of 20 mg/L, biochar of 3 g/L, rotation speed of 120 rpm, and reaction time of 50 min., at 26°C. Notably, the adsorbent had the maximum uranium removal effectiveness at pH 2.0, reaching 96.2%, as shown in Figure 4a. However, as the pH of the aqueous solution climbed from 2 to 10, the adsorption percentage decreased significantly, decreasing from 96.2% to 48.6%. The observed decrease in removal effectiveness was linked to increased pH levels. Because of the excellent uranium removal findings obtained at a pH of 2.0, this pH level was chosen as the preferable setting for all future adsorption tests.

The characteristics and ionic state of functional groups on the adsorbent and the specific chemical forms of uranium present in the solution impact the interaction between pH and uranium adsorption. In aqueous solutions with differing pH values, uranium takes on diverse forms. A fall in pH decreases the concentration of  $H^+$  ions on the adsorbent surface (Candamano et al, 2022). As a result, as indicated in the reference, the electrostatic attraction between the positively charged adsorbent surface and the negatively charged uranium ions becomes stronger. Higher pH values, on the other hand, exhibit electrostatic solid repulsion due to the presence of  $OH^-$  ions. The connection between pH and electrostatic interactions is critical in uranium adsorption.

#### **3.5 Impact of GE dose in uranium adsorption**

The study looked at the effect of changing the GE biochar dose from 0.5 g/L to 3.5 g/L at 0.5 g/L intervals. All other parameters remained constant, including pH, contact duration, uranium content, and temperature. The effect of activated biochar concentration on uranium adsorption is seen in Figure 4b. It is clear that as the adsorbent amount is lowered, uranium ion adsorption decreases gradually. Lower dose levels show a considerable lack of active sites, decreasing metal ion absorption from water. The adsorbent reduced uranium ions by 95.8% at the optimum biochar concentration of 3 g/L. Metal ion absorption plateaued at the 3 g/L threshold due to a decrease in the concentration gradient (Kaminski et al, 2015). The availability of an empty surface area during metal ion absorption by biochar aids in establishing the concentration gradient.

#### **3.6 Impact of ion concentration in uranium adsorption**

The findings on how the initial uranium concentration affects uranium removal by GE are shown in Figure 4c. As part of the inquiry on uranium removal via GE, variations in the initial ion concentration in an aqueous system were investigated, ranging from 10 to 50 mg/L. Temperature (26°C), pH (2), and contact time (60 minutes) were all kept constant. The curve in Figure 4c clearly shows that as the initial concentration of metal ions increases, the reduction in uranium decreases. According to the findings, the ideal concentration of metal ions for efficient adsorption is 20 mg/L. Lower metal ion concentrations have a comparatively more significant number of accessible adsorption sites, allowing for easier uranium ion adsorption (Kromah et al, 2021). In contrast, when the initial uranium ion concentration rises, the removal of uranium ions falls noticeably, owing to a decrease in the availability of adsorption sites.

### **3.7 Impact of contact time in uranium adsorption**

Figure 4d illustrates the impact of uranium ion adsorption as the contact time between activated charcoal GE powder and the synthetic solution varies from 10 to 60 minutes, maintaining an ion concentration of 20 mg/L. The ideal pH (2.0), GE dosage (3 g/L), ion concentration (20 mg/L), and temperature (26°C) parameters were addressed in this work, and the influence of modifications in contact duration was investigated. At the initial stage of the adsorption process, there is a high availability of active sites, leading to a rapid uptake of contaminants. As contact duration rises, the availability of active sites diminishes, resulting in less pollution pickup from the synthetic solutions (Benjelloun et al, 2021). After 50 minutes of contact time, the adsorbent's absorption of metal ions quickly diminishes, reaching a saturation point. As a result, most metal ion absorption occurs during the early phases of the adsorption process.

### **3.8 Impact of temperature in uranium adsorption**

By continuous heating, the temperature of the uranium ion-containing solution was increased from 15 to 60°C, and the impact was studied under optimal circumstances of pH 2.0, GE dosage 3 g/L, uranium concentration of 20 mg/L, and reaction time of 50 minutes. Figure 4e depicts the variations in adsorption efficiency when the temperature of the solution is changed. Uranium adsorption increased when the temperature rose to 30°C. However, as the temperature rose higher, metal ion absorption decreased. The decrease in adsorption efficiency with an increase in temperature was attributed to the faster desorption rate in the adsorption process (Sirusbakht et al, 2018).

### **3.9 Impact of particle size in uranium adsorption**

Various particle sizes (10, 25, 40, and 56 m) were used in batch mode to evaluate the effect of particle size on the adsorption process. Figure 4f demonstrates the changes in adsorption efficiency caused by differences in adsorbent particle size. The availability of surface area influences adsorption effectiveness, with smaller particle sizes giving a larger surface area. The figure illustrates that a

particle size of 10  $\mu\text{m}$  exhibited a high efficiency of 95.62%, and further increases in particle size resulted in a gradual decrease in adsorption efficiency. Furthermore, smaller particle sizes have fewer active sites, allowing for simple adsorbent particle attachment without surface contact (Yahya et al, 2020). This characteristic contributes to the higher efficiency of adsorption observed in smaller particle sizes.

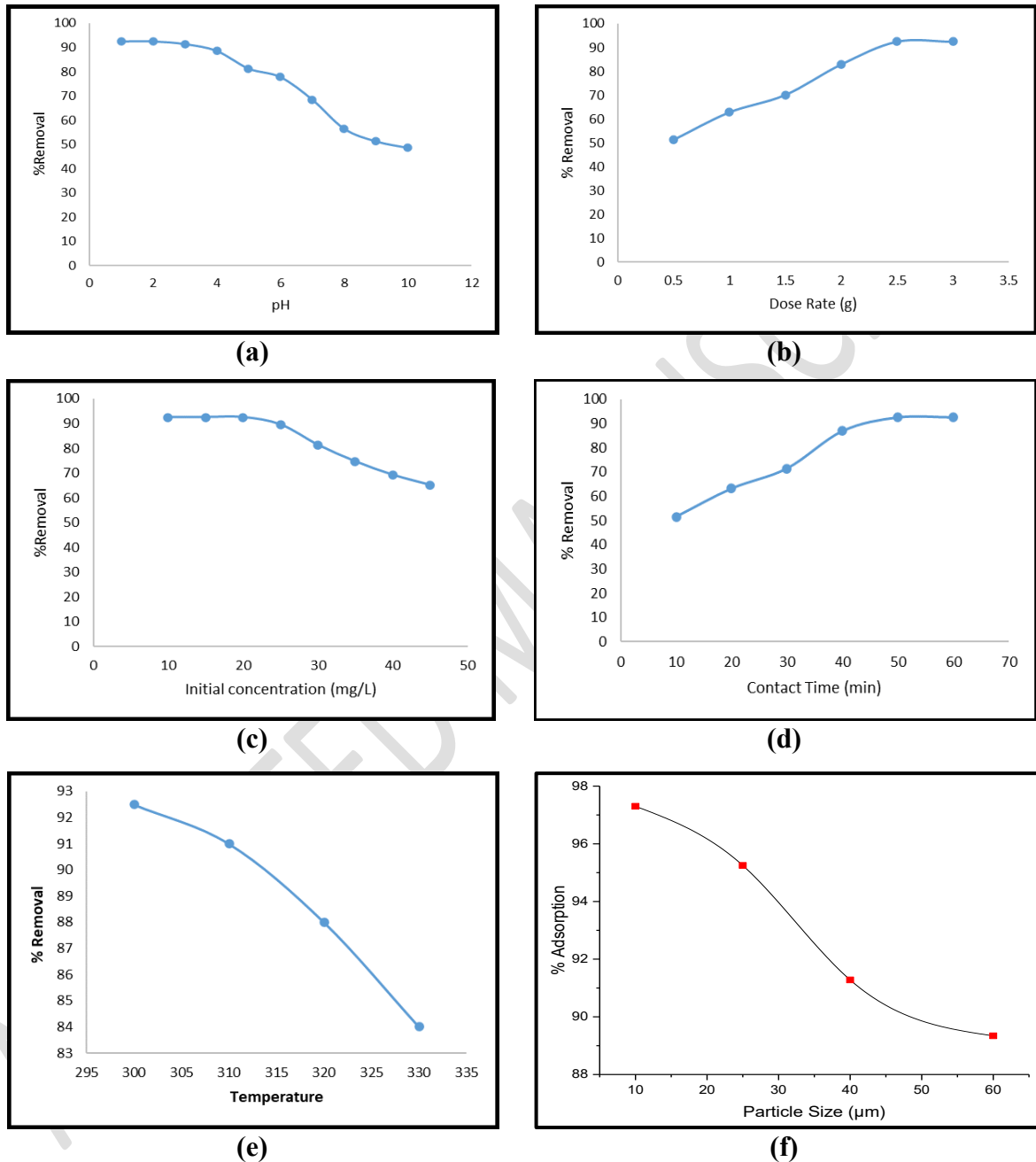


**Figure 4 (a), (b), (c), (d) & (e) - Impact of uranium adsorption by varying solution's pH, Biosorbent dose, Uranium concentration, Reaction time and Particle size respectively**

### 3.10 Modelling studies

The Langmuir isotherm model, represented in Figure 5a by the linear plot of  $C_e/q_e$  vs.  $C_e$  provides insights into the adsorption of molecules onto a surface. The equation for the Langmuir

isotherm involves parameters such as  $q_{\max}$  and  $K_L$ . The linear plot aids in determining these Langmuir parameters by assessing the slope and intercept. A separation parameter ( $R_L$ ) indicates the favorable adsorption process and the calculated value is within 0 to 1. The  $R^2$  value of 0.9764, exceeding 0.95, signifies a robust fit of the Langmuir isotherm model to the experimental data. This suggests that the adsorption process adheres to a heterogeneous monolayer mechanism and is deemed favourable (Regtil et al, 2017). The graphical representation of the Freundlich isotherm study is presented in Figure 5b, portraying the linear plot of  $\ln q_e$  against  $\ln C_e$ . This analysis allows the determination of parameters such as  $n$ , and  $K_f$ . The  $n$  value, calculated as 3.284, falling between 0 and 1, suggests a physical adsorption process by the GE biosorbent for uranium ions. Additionally, the regression value exceeding 0.95 indicates that the adsorption process involves a combination of both monolayer and multilayer adsorption, emphasizing the complexity of the adsorption mechanism (Hong et al, 2020).

The Dubinin-Radushkevich (D-R) isotherm model, utilized in this study, helps as an appreciated model to study the adsorption process and characterize the composition of the adsorbent material, specifically GE biochar at a temperature of 26°C. Figure 5c illustrates the plots generated by the D-R isotherm, with  $\ln q_e$  plotted against  $\epsilon^2$  (the Polanyi potential). This graphical representation aids in assessing the suitability of the D-R isotherm model for explaining the adsorption process. For a comprehensive understanding of the adsorption behaviour of metal ions on the GE biosorbent, Table 1 provides the essential constants derived from the D-R isotherm model. These constants play a crucial role in characterizing pollutant removal and gaining insights into the adsorption dynamics of metal ions on the GE biosorbent (Kołodzyńska et al, 2016). The evaluation of regression coefficient ( $R^2$ ) values serves as a crucial metric to assess the compatibility of the experimental data with the D-R isotherm model. When  $R^2$  values exceed 0.95, it indicates a strong alignment between the experimental data and the D-R isotherm model, implying that the model effectively elucidates the adsorption process. In the case of uranium metal ions, the obtained  $R^2$  values surpassing 0.95 signify a well-suited fit with the experimental model of the D-R study. This suggests that the D-R isotherm model accurately captures the intricacies of the uranium ion adsorption process on the GE biosorbent at the specified temperature of 26°C.

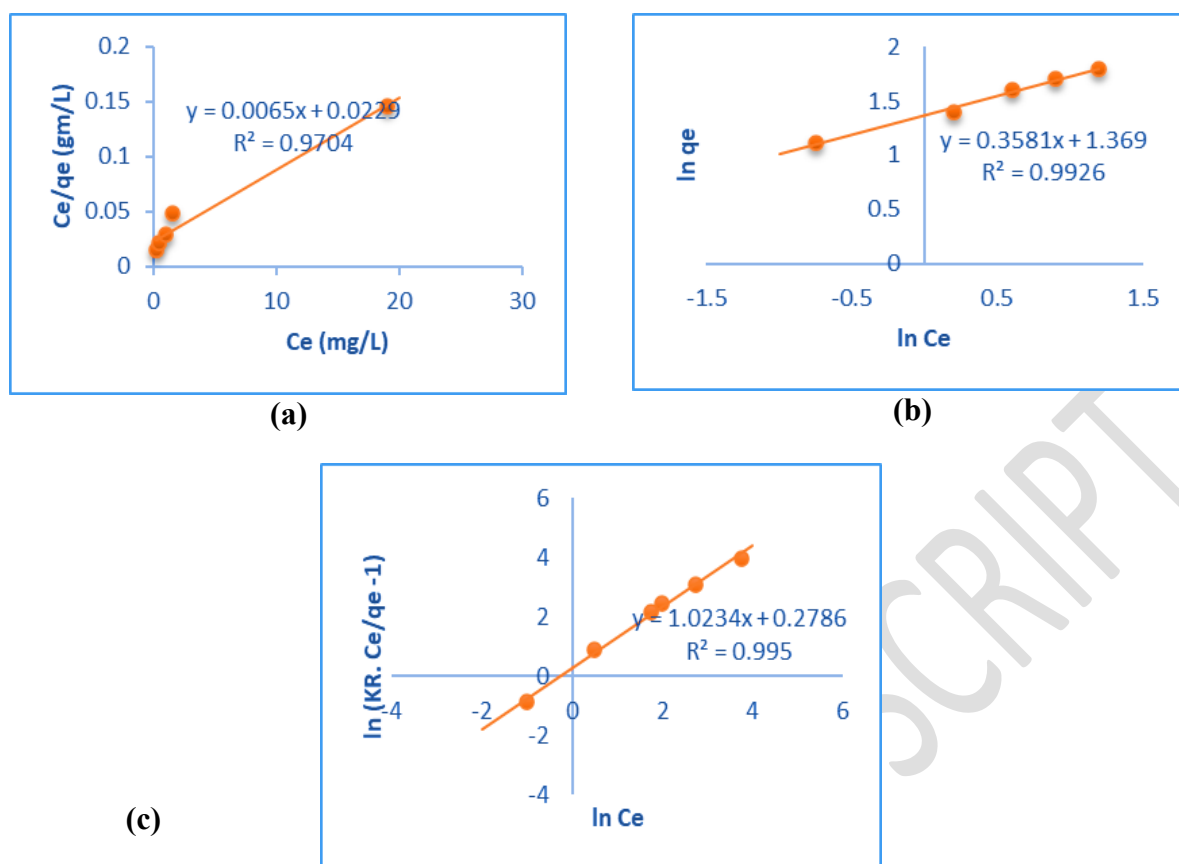


Figure 5 Equilibrium modelling plots for uranium adsorption using (a) Langmuir, (b) Freundlich and (c) D-R isotherm models

Table 1 Equilibrium constants for uranium adsorption using GE biosorbent

Type of model	Parameters	Units	U <sup>2+</sup>
Langmuir	q <sub>max</sub>	mg/g	12.19
	K <sub>L</sub>	l/mol	0.545
	R <sup>2</sup>	-	0.970
Freundlich	K <sub>f</sub>	L/g	4.031
	n	-	3.214
	R <sup>2</sup>	-	0.9926
D-R	X <sub>m</sub> × 10 <sup>-3</sup>	(mol/g)	4.64
	ε	KJ/mol	12.94
	R <sup>2</sup>	-	0.995

### 3.11 Kinetic studies

Figure 6a depicts the first-order kinetic model's linear plots [(q<sub>e</sub> - q) vs. t]. In studies where the metal ion concentration varied from 20 to 100 mg/L, the linear formulations of the first-order kinetic equation were employed. These formulations allowed the determination of the first-order rate

constant (k) along with the associated  $R^2$  values. The constants derived from this model were documented in Table 2, and the robust  $R^2$  values, surpassing 0.95, indicated the suitability and relevance of the Lagergren model for modelling the adsorption process. The high  $R^2$  values suggested that the adsorption process might have reached a saturation point under the given conditions. The model's ability to adequately replicate the experimental data shows that the adsorption process has achieved saturation (Manjuladevi et al, 2018). This kinetic model used the same uranium ion concentrations (20 to 100 mg/L) as the Pseudo-first-order investigations. This constant concentration range aided in the evaluation of employing activated biochar as an adsorbent for uranium ion adsorption. Figure 6b depicts this model's kinetic graphs ( $t/q$  vs.  $t$ ), and the relevant constants have been derived and reported in Table 2. Like the first-order investigations, the adsorption process constants showed a high connection with the pseudo-second-order kinetic model. Furthermore,  $R^2$  values greater than 0.95 demonstrate the relevance of this kinetic investigation. The pseudo- first and second-order models and their applicability suggest that the adsorption process has reached a saturation point in the removal of uranium ions from synthetic solutions (Batagarawa et al, 2019). This indicates that the adsorption capacity of the activated biochar material has been maximized under the specified experimental conditions.

The Elovich kinetic model and its fitting for the uranium adsorption have been evaluated by plotting the linear plot of  $qt$  vs  $\ln(t)$ . The regression value obtained from the plot for different concentrations of uranium metal ions was lower than the pseudo-first and second-order regression values. This lower value indicates the non-applicability of the Elovich kinetic model for uranium ion adsorption. Capturing the uranium ions using GE biosorbent was insignificant. The chemisorption process between the adsorbent and adsorbate has not led to the linear relationship ( $qt$  vs  $\ln t$ ), as seen in Figure 6c. However, the Elovich kinetic model can provide adsorption behaviour in a heterogeneous nature on the adsorbent surface (Phuengphai et al, 2021). Apart from the regression levels, the Elovich model provides valuable insight into the uranium ion adsorption using GE biosorbent in a heterogeneous nature.

**Table 2 Constants of adsorption kinetics for uranium removal using GE biosorbent**

S. No.	Conc. (mg/L)	Pseudo first order			Pseudo second order				Elovich		
		K ( $\text{min}^{-1}$ )	$q_e, \text{cal}$ (mg/g)	$R^2$	K (g/mg.min) $\times 10^{-3}$	$q_e, \text{cal}$ (mg/g)	h (mg/g.min)	$R^2$	a (mg/g.min)	b (g/mg)	$R^2$
1.	20	0.041	3.21	0.97	18.41	2.13	0.15	0.97	0.413	1.72	0.93
2.	40	0.059	7.04	0.95	15.38	5.48	0.17	0.95	0.854	0.95	0.92

3.	60	0.072	10.23	0.98	10.53	8.64	0.24	0.97	0.983	0.64	0.94
4.	80	0.063	13.82	0.97	6.49	10.84	0.27	0.96	0.942	0.41	0.92
5.	100	0.051	17.38	0.97	2.18	13.53	0.34	0.97	0.889	0.27	0.93

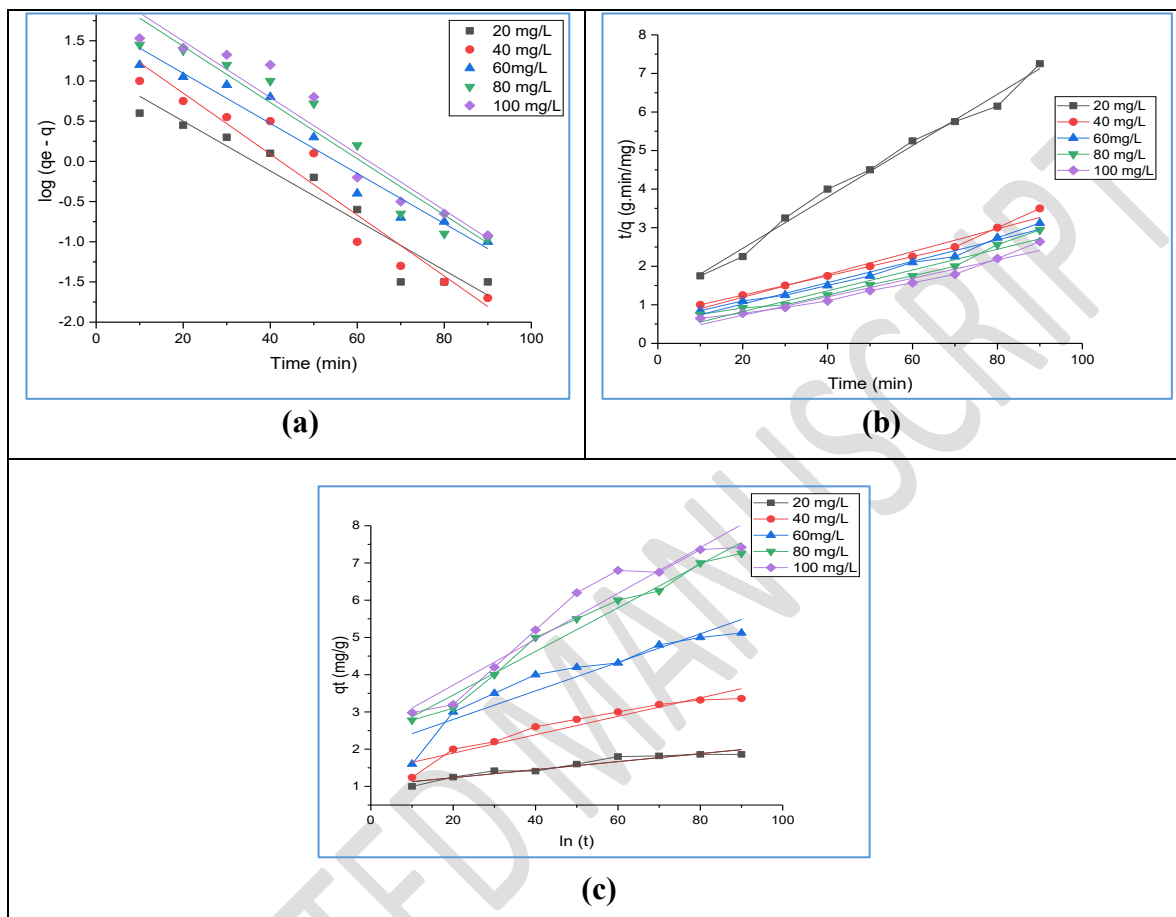


**Figure 6 Linear plots of kinetic models for uranium adsorption - (a) Pseudo – First order, (b) Pseudo-Second order and Elovich models**

### 3.12 pH – Zero-Point Change

The point of zero charge ( $pH_{PZC}$ ) represents the Columbia interaction between the adsorbent surface and the adsorbate in the liquid phase. As seen in Fig. 7, when adsorbent is added, the pH of the final solution increases until it hits the inversion point known as  $pH_{PZC}$ . The surface of activated carbons is protonated and acidic with positive charges at lower pH. Adsorption is impossible due to the electrical repulsion between uranium cations and the GE surface. Higher pH causes the surface to accumulate negative charges, resulting in electrostatic attraction (Saruchia et al, 2019). This discovery is supported by the FTIR, which shows enhanced surface basicity due to sulfuric acid activation and greater capacity at higher pH. The point of zero charge ( $pH_{PZC}$ ) for GE is 9.3 pH, indicating that the surface is primary; at 9.3 pH, the surface produces a net negative charge; higher solution pH favours uranium adsorption. The precursor is more acidic than primary groups, whereas GE contains more



basic than acidic groups, supporting the higher  $pH_{PZC}$ . Among acid groups, phenolic groups predominate (Ghayedi, et al, 2019). pH considerably impacts how an ion-molecule sticks to the adsorbent surface. pH influences the degree of uranium ionisation and the dissociation of functional groups on the carbon surface.

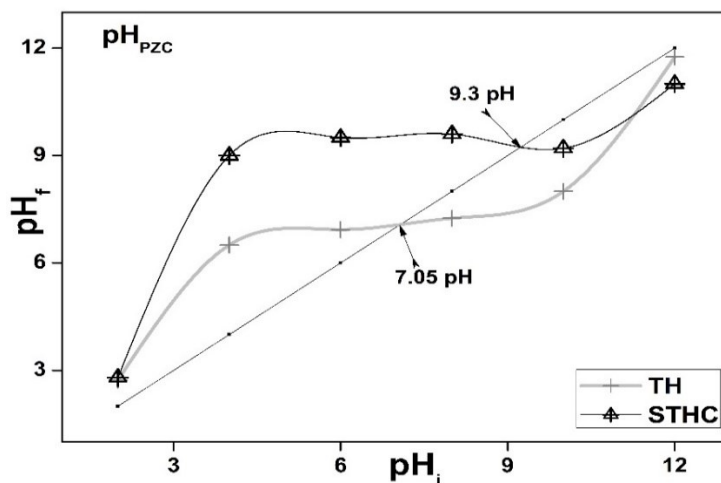


Figure 7  $pH_{ZPC}$  of the biosorption of uranium using GE

### 3.13 Thermodynamics of uranium ion adsorption

The uranium ions and their concentration were varied in different experimental conditions and their thermodynamics were investigated. The thermodynamic plot for uranium ion adsorption is shown in Figure 8 for the corresponding ion concentrations. The computed slope and intercept values ( $H_o$  and  $S_o$ ) are shown in Table 3. The process is endothermic due to the spontaneous nature of the GE biosorbent, as demonstrated by the negative  $G_o$  (Gibbs Energy) and positive  $H_o$  (Enthalpy) values. The positive entropy values and their increments signify an increase in disorder during the adsorption of a substance in an aqueous medium, indicating a transition or interaction between the solid adsorbent and the liquid solution (Wang et al, 2022).

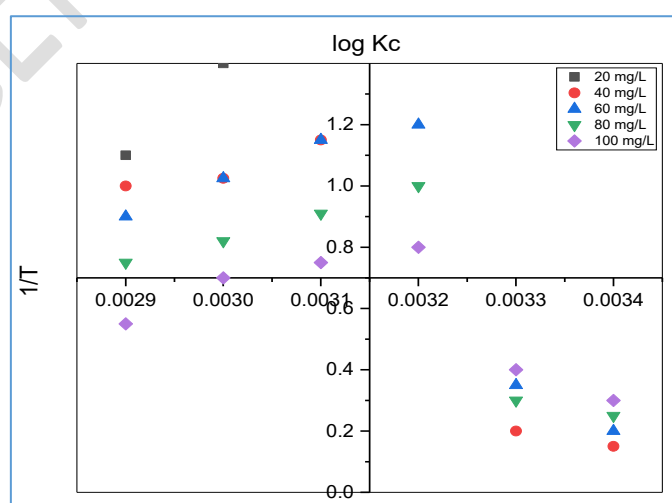


Figure 8 Thermodynamic plot of uranium ion adsorption using GE biosorbent

**Table 3 Thermodynamic constants of uranium adsorption**

Initial concentration of Uranium ions	Enthalpy ( $\Delta H^\circ$ ) KJ/mol	Entropy ( $\Delta S^\circ$ ) J/mol	Gibbs Energy ( $\Delta G_0$ ) kJ/mol			
			15°C	30°C	45°C	60°C
20	85.064	192.348	-15.640	-11.641	-9.649	-8.162
40	47.651	100.658	-12.894	-9.942	-7.645	-5.614
60	24.756	55.592	-10.971	-7.987	-5.692	-4.093
80	18.974	30.437	-8.697	-5.953	-3.564	-2.952
100	14.687	25.646	-5.987	-4.094	-2.651	-1.926

### 3.14 Desorption experiment

Using concentrated sulfuric acid at concentrations ranging from 0.1 to 0.4 N, the GE biosorbent efficiently released uranium ions that had been adsorbed in the elution studies. The retrieval of uranium metal ions increased significantly when the sulfuric acid concentration was increased to 0.3 N. However, when the sulfuric acid concentration grew, the uranium recovery decreased. the addition of 0.3 N H<sub>2</sub>SO<sub>4</sub> is effective in recovering uranium ions from the spent adsorbent, and the process reaches a saturation point where further increases in desorbing agent concentration do not lead to additional recovery (Xi et al, 2020). This indicates the completion of the desorption process. In this research, the utilization of 0.3 N H<sub>2</sub>SO<sub>4</sub> led to the successful recovery of 93.27% of uranium ions from the used adsorbent. This demonstrates the efficacy of the desorption process using 0.3 N H<sub>2</sub>SO<sub>4</sub> in reclaiming uranium ions from the spent adsorbent for further analysis or applications.

### CONCLUSION

The uranium ion biosorption was studied utilizing activated *Gracilaria Edulis* seaweed as the adsorbent. Batch tests found excellent parameters, including a pH of 2.0, a GE dose of 3 g/L, and an ideal uranium concentration of 20 mg/L at 26°C. The developed biosorbent material showed exceptional adsorption ability, removing 91.27% of uranium ions from synthetically created solutions. Isothermal investigations using the Langmuir and Freundlich models revealed a multilayered and heterogeneous adsorption mechanism that corresponded well with batch adsorption. Kinetic investigations, including pseudo-first and second-order models, showed that metal ion absorption by the adsorbent included external film diffusion via physical and chemical mechanisms. Thermodynamic analyses revealed that uranium ion adsorption is endothermic. Distant landfills effectively handle pollutants. In conclusion, this experimental investigation demonstrates the efficacy of *Gracilaria Edulis* seaweed in eliminating contaminants from aqueous solutions.

## REFERENCES

- A.K. Priya, V. Yogeshwaran, Saravanan Rajendran, Tuan K.A. Hoang, Matias Soto-Moscoco, Ayman A. Ghfar and Chinna Bathula (2022). Investigation of mechanism of heavy metals ( $\text{Cr}^{6+}$ ,  $\text{Pb}_2+$  &  $\text{Zn}^{2+}$ ) adsorption from aqueous medium using rice husk ash: Kinetic and thermodynamic approach, *Chemosphere*, 286, 131796. <https://doi.org/10.1016/j.chemosphere.2021.131796>
- Abdelmajid Regti1, My Rachid Laamari, Salah-Eddine Stiriba and Mohammadine El Haddad (2017). The potential use of activated carbon prepared from *Ziziphus* species for removing dyes from waste waters. *Applied Water Science*, 7, 4099 – 4108. Doi: <https://doi.org/10.1007/s13201-017-0567-8>
- Ahmed Eleryan, Uyiosa O. Aigbe, Kingsley E. Ukhurebor, Robert B. Onyanacha, Tarek M. Eldeeb, Mohamed A. El-Nemr, Mohamed A. Hassaan, Safaa Ragab, Otolorin A. Osibote, Heri S. Kusuma, Handoko Darmokoesoemo and Ahmed El Nemr (2022). Copper(II) ion removal by chemically and physically modified sawdust biochar. *Biomass Conversion and Biorefinery*. <https://doi.org/10.1007/s13399-022-02918-y>
- Amit Kumar Dey, Abhijit Dey and Rumi Goswami (2022). Adsorption characteristics of methyl red dye by  $\text{Na}_2\text{CO}_3$ -treated jute fibre using multi-criteria decision-making approach, *Applied Water Science*, 12, 179. <https://doi.org/10.1007/s13201-022-01700-9>
- Batagarawa SM, Ajibola AK (2019). Comparative evaluation for the adsorption of toxic heavy metals on to millet, corn and rice husks as adsorbents. *Journal of Analytical and Pharmaceutical Research*, 3, 119-125. Doi: [10.15406/japlr.2019.08.00325](https://doi.org/10.15406/japlr.2019.08.00325)
- Chuanbin Wang, Xutong Wang, Ning Li, Junyu Tao 2, Beibei Yan, Xiaoqiang Cui and Guanyi Chen (2022). Adsorption of Lead from Aqueous Solution by Biochar: A Review. *Clean Technologies*, 4, 629 – 652. <https://doi.org/10.3390/cleantechnol4030039>
- Dorota Kołodyńska, Justyna Bąk and P. Thomas (2016). Comparison of Sorption and Desorption Studies of Heavy Metal Ions from Biochar and Commercial Active Carbon. *Chemical Engineering Journal*, 307. Doi: <http://dx.doi.org/10.1016/j.cej.2016.08.088>
- Jatinder Singh, Neha Dhiman and Neeta Kapur Sharma (2018). Effect of Fe(II) on the Adsorption of Mn(II) from Aqueous Solution Using Esterified Saw Dust: Equilibrium and Thermodynamic Studies. *Indian Chemical Engineer*, 60 (3), 255 – 268. <https://doi.org/10.1080/00194506.2017.1363674>
- Jayachandran Sheeja, Krishnan Sampath and Ramasamy Kesavasamy (2021). Experimental Investigations on Adsorption of Reactive Toxic Dyes Using *Hedyotis umbellata* Activated Carbon, *Adsorption Science and Technology*, ID – 5035539. <https://doi.org/10.1155/2021/5035539>

- Jie Hong, Junyu Xie, Seyyedali Mirshahghassemi, Jamie Lead (2020). Metal (Cu, Cr, Ni, Pb) removal from environmentally relevant waters using polyvinylpyrrolidone – coated magnetic nanoparticles. *RSC advances*, 10, 3266 – 3276. Doi: <https://doi.org/10.1039/C9RA10104G>
- Liangjun Xi, Sijie Zhou, Chunhua Zhang, Zhuan Fu, Aming Wang, Qian Zhang, Yunli Wang, Xin Liu, Xungai Wang and Weilin Xua (2020). Environment-friendly *Juncus effusus*-based adsorbent with a three-dimensional network structure for highly efficient removal of dyes from wastewater, *Journal of Cleaner Production*, 259, 120812. <https://doi.org/10.1016/j.jclepro.2020.120812>
- Long Su, Haibo Zhang, Kokyo Oh, Na Liu, Yuan Luo, Hongyan Cheng, Guosheng Zhang and Xiaofang He (2021). Activated biochar derived from spent *Auricularia auricula* substrate for the efficient adsorption of cationic azo dyes from single and binary adsorptive systems, *Water Science & Technology*, 84 (1), 101 – 121. <https://doi.org/10.2166/wst.2021.222>
- Manjuladevi M, Anitha R, Manonmani S (2018). Kinetic study on adsorption of Cr (VI), Ni (II), Cd (II) and Pb (II) ions from aqueous solutions using activated carbon prepared from cucumis melo peel. *Applied water science*, 8, 36. Doi: <https://doi.org/10.1007/s13201-018-0674-1>
- Melânia Feszterová, Lýdia Porubcová and Anna Tirpáková (2021). The Monitoring of Selected Heavy Metals Content and Bioavailability in the Soil-Plant System and Its Impact on Sustainability in Agribusiness Food Chains, *Sustainability*, 13, 7021. <https://doi.org/10.3390/su13137021>
- Mohammed Benjelloun, Youssef Miyah, Gulsun Akdemir Evrendilek, Farid Zerrouq Sanae Lairini (2021). Recent Advances in Adsorption Kinetic Models: Their Application to Dye Types, *Arabian Journal of Chemistry*, 14 (4), 103031. <https://doi.org/10.1016/j.arabjc.2021.103031>
- Nadir Khan, Fazal Wahid, Qamar Sultana, Najm Us Saqib and Muhammad Rahim (2020). Surface oxidized and un-oxidized activated carbon derived from *Ziziphus jujube* Stem, and its application in removal of Cd (II) and Pb (II) from aqueous media. *SN Applied Sciences*, 2, 753. Doi: <https://doi.org/10.1007/s42452-020-2578-6>
- Narjes Ghayedi, Jaleh Mohajeri Borazjani and Dariush Jafari (2019). Biosorption of arsenic ions from the aqueous solutions using *Chlorella vulgaris* micro algae, *Desalination and Water Treatment*, 165, 188 – 196. [doi:10.5004/dwt.2019.24445](https://doi.org/10.5004/dwt.2019.24445)
- Nathalia Krummenauer Haro, Ivone Vanessa Jurado Dávila, Keila Guerra Pacheco Nunes, Marcela Andrea Espina de Franco, Nilson Romeu Marcilio and Liliana Amaral Féris (2021). Kinetic, equilibrium and thermodynamic studies of the adsorption of paracetamol in activated carbon in batch model and fixed-bed column, 11 (38). <https://doi.org/10.1007/s13201-020-01346-5>
- Pongthipun Phuengphai, Thapanee Singjanusong, Napaporn Kheangkhun, Amnuay Wattanakornsiri, Removal of copper (II) from aqueous solution using chemically modified fruit peels as efficient

- low-cost biosorbents. *Water Science and Engineering.*, 14 (4) (2021), 286 – 294.  
<http://dx.doi.org/10.1016/j.wse.2021.08.003>
- Qian Wang, Liping Liang, Fenfen Xi, Gangliang Tian, Qiaole Mao and Xu Meng (2020). Adsorption of Azo Dye Acid Red 73 onto Rice Wine Lees: Adsorption Kinetics and Isotherms, *Advances in Materials Science and Engineering*, ID – 3469579. <https://doi.org/10.1155/2020/3469579>
- S. Candamano, A. Policicchio, G. Conte, R. Abarca, C. Algieri, S. Chakraborty, S. Curcio, V. Calabrò, F. Crea and R.G. Agostinobc (2022). Preparation of foamed and unfoamed geopolymer/NaX zeolite/activated carbon composites for CO<sub>2</sub> adsorption, *Journal of Cleaner Production*, 330, 129843. <https://doi.org/10.1016/j.jclepro.2021.129843>
- Samin Sirusbakht, Leila Vafajoo, Samira Soltani, Shahriar Habibi (2018). Sawdust Bio sorption of Chromium (VI) Ions from Aqueous Solutions. *Chemical Engineering Transactions*, 70, 1147 – 1152. [10.3303/CET1870192](https://doi.org/10.3303/CET1870192)
- Saruchia, Vaneet Kumar, Adsorption kinetics and isotherms for the removal of rhodamine B dye and Pb<sup>+2</sup> ions from aqueous solutions by a hybrid ion-exchanger. *Arabian Journal of Chemistry.*, 12 (3) (2019), 316 – 329. <https://doi.org/10.1016/j.arabjc.2016.11.009>
- Serdar Aydina, Hamda Mowlid Nura, Abdoulaye Mamadou Traorea, Eren Yildirim and Serkan Emik (2021). Fixed bed column adsorption of vanadium from water using amino-functional polymeric adsorbent, *Desalination and Water Treatment*, 209, 280 – 288. [10.5004/dwt.2021.26493](https://doi.org/10.5004/dwt.2021.26493)
- T. G. Ambaye, M. Vaccari, E. D. van Hullebusch, A. Amrane and S. Rtimi (2021). Mechanisms and adsorption capacities of biochar for the removal of organic and inorganic pollutants from industrial wastewater, *International Journal of Environmental Science and Technology*, 18, 3273 – 3294. <https://doi.org/10.1007/s13762-020-03060-w>
- Varney Kromah and Guanghui Zhang (2021). Aqueous Adsorption of Heavy Metals on Metal Sulfide Nanomaterials: Synthesis and Application, *Water*, 13 (13), 1843. <https://doi.org/10.3390/w13131843>
- Wladyslaw Kaminski, Elwira Tomczak and Pawel Tosik (2015). Kinetics of azo dyes sorption onto low-cost sorbents, *Desalination and Water Treatment*, 55, 2675 – 2679. <https://doi.org/10.1080/19443994.2014.958276>
- Wojciech Konicki, Małgorzata Aleksandrak, Dariusz Moszyński and Ewa Mijowska (2017). Adsorption of anionic azo-dyes from aqueous solutions onto graphene oxide: Equilibrium, kinetic and thermodynamic studies, *Journal of Colloid and Interface Science*, 496, 188 – 200. <https://doi.org/10.1016/j.jcis.2017.02.031>

- Xiaoran Zhang, Shimin Guo, Jungfeg Liu, Ziyang Zhang, Kaihong Song, Chaohong Tan, Haiyan Li (2019). A study on the removal of copper (II) from aqueous solution using lime sand bricks. *Applied Sciences*, 9 (4), 670. Doi: <https://doi.org/10.3390/app9040670>
- Y. Venkatraman and A.K. Priya (2021). Removal of heavy metal ion concentrations from the wastewater using tobacco leaves coated with iron oxide nanoparticles, *International Journal of Environmental Science and Technology*, 19, 2721–2736. <https://doi.org/10.1007/s13762-021-03202-8>
- Yahya M.D, Aliyu A.S, Obayomi K.S, Olugbenga A.G, Abdullahi U.B (2020) Column adsorption study for the removal of chromium and manganese from electroplating wastewater using cashew nutshell adsorbent. *Chemical engineering* 7 : 1748470. Doi: <https://doi.org/10.1080/23311916.2020.1748470>